MIDDLE EAST TECHNICAL UNIVERSITY

Investigation of Neutrino's Role in Non-Invasive Medical Diagnostics

Abdullah Burkan Bereketoglu
Recep Durna

Department of Physics

Phys 408: Particle Physics II - Term Project

Instructor: Prof. Dr. Ismail Turan

Abstract

Recent studies in nuclear physics on medical physics applications show a search for more abundant sources without energy consumption while providing better detail in images from their interactions are looking for. As it is known neutrinos are such particles that have high penetrability, with approximately 100 trillion neutrinos passing each human body every second. However, its weak interacting behavior with matter makes the detection of them really difficult, therefore to detect their trace. Nevertheless, recent developments in the detection of neutrinos as technology has opened new frontiers for their possible usage in medical imaging. Even though it is still not that promising, since it does not seem feasible to use neutrinos to create images from small beings such as humans compared to celestial bodies, it is possible to analyze the possible frontiers for neutrino usage other than celestial tomography, by tools such as GEANT4. The paper hereby aims to provide simulation analysis with theoretical background knowledge to find pathways to achieve the goal of the feasible application of neutrino tomography in the medical domain. To accomplish it, the paper aims to explore novel particle imaging tools, such as PET, and SPECT, and show the performance of how neutrinos perform in similar domains. Tissue-like materials were investigated by simulation on GEANT4 and explored the detectability of neutrinos after penetrating tissue-like materials. Results are discussed to see the future usage of neutrinos in the medical domain.

Contents

1 Introduction

Currently, the most prominent medical imaging systems are Positron Emission Tomography (PET) and Single-Photon Emission Computerized Tomography (SPECT) imaging systems. [2] In PET, the positron is sent to the tissue, and it annihilates with an electron near rest creating two anti-parallel photons. The response line is determined from the simultaneous detection of photons from two opposing detectors. Analysis of the detections' timings gives the image's exact position. In SPECT, radioactive decay of nuclei is utilized to generate gamma, a single photon in the tissue. Then, the parallel photons are detected with the help of collimators. Projections are generated for different angles to obtain the full image. However, medical imaging systems are constantly evolving, and new systems emerge with the application of discoveries into the principle.

In the literature, neutrino tomography is an emerging field, especially for the determination of the density profile of the earth. Two main tomography methods are discussed with the neutrinos: neutrino oscillation tomography [4, 5, 6, 7] or neutrino absorption tomography [8]. Also, its practical applications for nuclear security are discussed in [3, 9]. Neutrinos can be utilized in tomography for practical applications due to their abundance despite their weakly interacting nature. Here in the study, it is discussed whether it will be appropriate to use neutrinos for small-material imaging such as the human body. Theoretically, it is expected that neutrinos won't make any interaction even in the entire lifetime of a human being[11].

2 Properties of Neutrinos

2.1 Propagation of neutrino in matter

The transverse of neutrinos through matter is determined by the four main contributions: (1) the standard evolution Hamiltonian for neutrino oscillations, (2) the attenuation effect by inelastic interactions of the neutrino with the matter, either via charged-current or neutral-current processes, (3) the redistribution of neutrinos from higher to lower energies after neutral-current interactions, and (4) the regeneration of neutrinos from tau lepton decays. For smaller energies below a few hundred GeV, neutrino flavor oscillations are the dominant contributions. To the contrary, the other terms start to dominate for higher energies. The cross-section of neutrino nucleon increases with energy, so the neutrino flux gets attenuated at high energies. Moreover, tau lepton decays generate secondary neutrinos. For some selected energies, the attenuation effect is dominant, neutrino oscillations are suppressed, and the secondary regenerated neutrinos from tau lepton decays are negligible.

The attenuation of the neutrino flux is governed by the interaction and absorption mechanisms. In our work, to simulate the absorption of neutrino through matter Geant4 is employed, which is a platform for the simulation of the passage of particles through matter using Monte Carlo methods.

The neutrino flavor oscillations are discovered with atmospheric and solar neutrinos; subsequently, they are verified using reactor and accelerator neutrinos. [5] Therefore, neutrinos are massive particles that are a mix of mass eigenstates. In the Standard Model, known states $|\nu_\alpha\rangle$ for $\alpha = e, \mu, \tau$ are linear combinations of mass states $|\nu_i\rangle$ with masses m_i for $i = 1, 2, 3$. This can be represented by a unitary mixing matrix U with $|\nu_\alpha\rangle = \sum_i U^*_{\alpha i} \, |\nu_i\rangle$ and

$$U = O_{23}\Gamma O_{13}\Gamma^\dagger O_{12} \tag{1}$$

where O_{ij} are orthogonal matrices representing rotations by mixing angles θ_{ij}, and $\Gamma = \mathrm{diag}(1, 1, e^{i\delta})$ is a complex diagonal matrix responsible from the CP violation in weak interactions. In addition to these, mass-squared differences, $\Delta m^2_{21} \equiv m^2_2 - m^2_1$ and $\Delta m^2_{31} \equiv m^2_3 - m^2_1$, parametrize the neutrino oscillations. The sign of Δm_{31} is not known, which leads to two possible mass hierarchies, normal and inverted mass hierarchies. The solar oscillation parameters, Δm^2_{21}, θ_{12}, and the atmospheric oscillation parameters, Δm^2_{31}, θ_{23} are determined from the experiments. However, only an upper limit exists for θ_{13} [10], and information about complex phase δ_{CP} is not yet available.

Neutrinos can be produced and detected in flavor eigenstates. However, neutrinos oscillate between different flavor states due to different mass eigenstates along the trajectory. Then, the probability of a flavor eigenstate α to change into flavor eigenstate β at a distance L from the source such that

$\nu_\alpha \to \nu_\beta$ is given as

$$P_{\alpha\beta} = |\,\mathcal{U}_{\beta\alpha}|^2 \quad \text{with} \quad \mathcal{U}_{\beta\alpha} = \langle\nu_\beta|\,\hat{\mathcal{U}}\,|\nu_\alpha\rangle \tag{2}$$

where the probability amplitude $\mathcal{U}_{\beta\alpha}$ is an element of the unitary evolution operator matrix $\mathcal{U}$ in the flavor basis. In the limit of two flavor case, the oscillation probability $\nu_\alpha \to \nu_\beta$ in the vacuum is

$$P_{\alpha\beta} = \sin^2(2\theta)\sin^2\left(\frac{\Delta m^2 L}{4E}\right) \tag{3}$$

where θ is the mixing angle of a 2×2 rotation matrix U between α and β states, Δm^2 is the mass-squared difference, E is the energy of the neutrino, and L is the length of the baseline, the distance between source and detector. Also, the probability of flavor conservation is given by $P_{\alpha\alpha} = 1 - P_{\alpha\beta}$. However, the real picture with three neutrino flavors is much more complicated.

Moreover, neutrino flavor oscillations are affected by the presence of matter due to the abundance of electrons. Interactions of electron neutrinos with electrons and nucleons lead to coherent forward scattering in matter. This matter effect is added as a potential term to the evolution Hamiltonian, $H(L)$ which characterizes the oscillations. This potential term is $V(L) = \mp \mathrm{v}(L)\mathrm{diag}(1,0,0)$ with $\mathrm{v}(L) = \sqrt{2}G_F\ n_e(L)$. Here, minus sign refers to neutrinos, and plus sign refers to antineutrinos, and G_F is the Fermi constant. The electron number density is given with regard to matter density as

$$n_e(L) = \frac{Z}{A}\frac{\rho(L)}{m_N} \tag{4}$$

where m_N is the nucleon mass and Z/A can be approximated as 0.5 for stable heavy nucleons. In the limit of two flavor case Hamiltonian becomes

$$H(n_e) = U\begin{bmatrix} 0 & 0 \\ 0 & \frac{\Delta m^2_{21}}{2E} \end{bmatrix} U^\dagger + \begin{bmatrix} \pm\mathrm{v}(n_e) & 0 \\ 0 & 0 \end{bmatrix} \tag{5}$$

2.2 Detection approaches to use for neutrino tomography

There are two main possible methods of tomography with neutrinos: neutrino absorption tomography and neutrino oscillation tomography. Moreover, there is another possible method called neutrino diffraction tomography that is rare and will not be explicitly discussed. [4]

In neutrino absorption tomography, the image can be reconstructed by measuring the attenuation of the neutrino flux since they are absorbed along the media. The image reconstruction of the object is done with the help of measured absorption rates of neutrinos passing through the object from different angles. At high energies, neutrino cross-sections are increased enough to be detected, even though they are weakly interacting.

In neutrino oscillation tomography, the density profile is reconstructed from the matter effects on the flavor oscillations. The matter density affects the flavor oscillation probabilities and determines the ingoing and outgoing neutrino flavors. Therefore, the image can be reconstructed from the measured neutrino flavors.

3 Physical Principles of Medical Imaging Systems

In emission tomography, a medical imaging technique, radioisotopes are injected into the body to measure the regional tissue by detecting the radiation emitted from the radioisotopes.

3.1 Positron Emission Tomography (PET)

Positrons, positively charged anti-electrons, are emitted from the radioactive decay of a proton-rich nucleus. In this process, the energy of the emitted positrons is a continuous spectrum up to a maximum energy. After emission, the positron loses its kinetic energy through interactions with matter, and it is deflected from its original path throughout the process. Ultimately, the positron meets an electron at rest and annihilates into two photons in anti-parallel directions. Simultaneous detection of these two opposing photons defines the line of response. Uncertainties in the final momentum of the positron and simultaneity of detection decrease the localization power and spatial resolution. The detection of photons is accomplished using gamma cameras. Also, in the detection of the photons, photomultiplier tubes (PMTs) are utilized to increase the intensity of the photons, which increases the noise.

3.2 Single-Photon Emission Computerized Tomography (SPECT)

Radioactive decay is a natural process in which the unstable nucleus of an atom releases energy through the spontaneous emission of ionizing radiation. Radioisotopes or radionuclides are unstable nuclei that exhibit the property of radioactive decay, which is either natural or artificial. Technetium-99m is frequently utilized in nuclear medicine, which decays into Technetium-99 by emitting gamma rays of 140 keV of energy. It is preferred due to its on-site availability thanks to the the longer-lived Molybdenum-99 from which Technetium-99m can be produced, and its energy is in the ideal range for efficient detection.

Unlike PET, single-photon detection utilizes physical collimation to acquire directional information about incident photons. The detection of photons is accomplished using a gamma camera, and the active component of the detector head is typically a large scintillation crystal. This crystal is capable of recording the incident photons that have not been absorbed by

the physical collimator placed in front of it. The collimator ensures the recorded photons are parallel by absorbing photons in other directions. It is made of materials with a high probability of interaction with the photons, such as lead or tungsten. It comprises a large number of holes to allow the passage of incident photons only in the direction parallel to the holes. In single-photon emission tomography (SPECT), a gamma camera acquires a series of planar projections at different angles around the patient to derive transverse images revealing the distribution of activity within the body.

Photons emitted from areas of radiopharmaceutical uptake at different depths within the body, can undergo various interactions with matter. It can be either attenuated, which leads to an underestimation of activity concentration. However, photon scattering leads to a change in photon direction. The photon scatter effect is a background-like phenomenon that often overestimates activity concentration in regions with low uptake. Several methods have been utilized to perform attenuation and scatter correction. Moreover, photomultiplier tubes (PMTs) are used to detect the photons, increasing the noise.

4 Neutrino Tomography: Its Limitations and Feasability

Neutrino interaction, like any interaction, depends on certain variables. In the neutrino case, it can be said that it requires a massive matter, high flux, which for neutrino is easily obtained, and high energy for small masses at short periods, for long periods, higher effective cross-sections may be required. For neutrino absorption tomography [7]

$$\frac{\sigma}{E} = 10^{-35}\frac{cm^2}{TeV} \tag{6}$$

We assume the flux is $\phi = 1\frac{neutrino}{cm^2*s}$ with that for an average human being, it is impossible to see even 1 interaction in its entire lifespan. however, for a massive object, let's say earth, which is 5.972 * 10^{24} kg mass, which is approximately 10^{50} atoms, then the calculation becomes for a 1 TeV neutrino:

$$1\frac{neutrino}{cm^2*s}*1TeV*10^{-35}*0.95\frac{cm^2}{TeV}*10^{50}atoms*1s = 9.5*10^{14}interactions \tag{7}$$

The above equation shows that for a massive object, it is highly probable that neutrino interacts with the mass. Over an extended period, it can indicate a good image resolution from an abundant neutrino source. One can consider the 7*10^{27} atoms in an average human body and think it is not enough for 1 neutron flux per centimeter-square to make any interaction.

4.1 Limitations

1. Not useful for non-massive objects
2. Resolution gain takes much time due to interaction, and returning particle traces are relatively low
3. Hard to determine the track of one neutrino, which is hard to make accurate imaging at short and even in long-time without precision calibration.

4.2 Feasibilities

1. It is abundant, therefore, if correct tools are designed, they can make cheap and long-serving data collection tools for distant celestials and astrophysical structures.
2. It does not require too much handling during data collection, make it sit still, and it will collect.

5 GEANT4 simulation of neutrino

GEANT4 is a simulation tool developed for nuclear-medical-particle physicists and carries high-level programming and statistics knowledge. GEANT4, in essence, simulates the passage of particles through matter. GEANT4 uses various areas, including particle collisions, geometry design, decay observations, dosimetry, microelectronics, calorimetry, biological physics, medical physics, nuclear physics imaging, radiation, and other interdisciplinary nuclear physics-related simulation-based experimentations.

Geant4 is used for biological tissue-like imaging and absorption imaging analysis in this project.

5.1 Design of the simulation

Specific parameters must be considered in the design of the simulation via GEANT4. One of which is the geometry of the designated phantom. For a whole human body, different body organs should be shown with different geometry, such as spherical, paraboloid, ellipsoid, ellipsoid tube, subtraction solid, and more special cases. Also, different types of elemental composition for each tissue must be made to make a fully designed phantom.

Later, when the phantom is put into the designed physical world, we will implement our particle gun, where it is located, with how many beams are shot. Volumes should be defined, positioning of the gun from half(x,y,z), center, and how its direction in the world will behave. In the experimentation, we used ν_e as our primary particle.

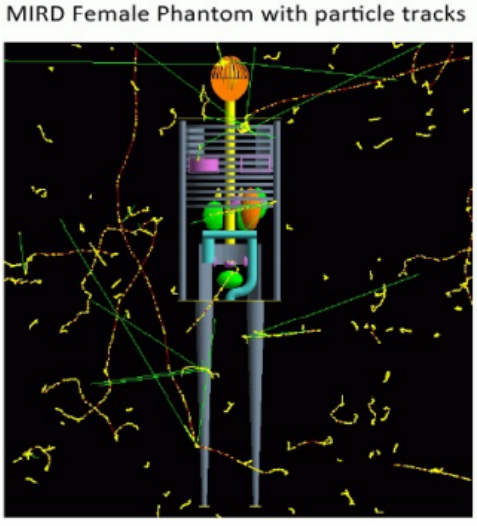

Figure 1: MIRD Female Phantom in GEANT4 design

Lastly, flux scorers are designed and embedded into each geometry to an-

alyze the energy depositions. Flux deposition gives us the particle difference due to the absorbed particle count at each geometry and tissue.

5.2 Material selection for tissue-like absorbers

For the primitive GEANT4 simulation design, the selected geometry is a flat 3-D rectangle, the default geometry in GEANT4. If the $x - y - z$ coordinate space is not equal, it is rectangular, not cubical. For selecting the material for tissue-like absorbers, one can either design a tissue with specific carbon, nitrogen, oxygen, and other elements in the mixture or select already available GEANT4 materials from the material library. In GEANT4, a NIST library is the short version of the National Institute of Standards and Technology. The NIST database consists of materials from soft tissues to precious metals. In our primitive simulation design, ICRP and NIST database mixture G4-SOFT-TISSUE-ICRP is used. ICRP stands for International Commission on Radiological Protection which added specific characteristics to the soft tissue material of the NIST database.

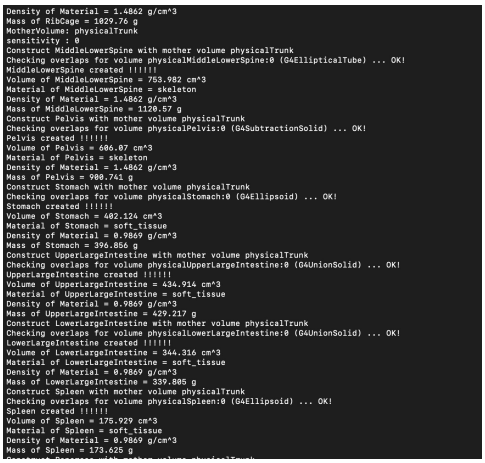

Figure 2: Tissue structures, densities, volumes, and geometries

Therefore, for material selection to construct tissue-like absorbers, it is one either needs to make a realistic atomistic composition-based material with characteristic geometry and volume as used in the simulation with human phantom, or one can use readily available materials which are specifically designed for such experimentations via experts of the case at NIST and ICRP.

As shown above, one can model and parameterize the ν_e in a primitive way that gives an opinion about how a neutrino simulation is conducted via GEANT4.

(a) Primitive GEANT4 Detector construction

(b) Primitive GEANT4 PGS

(c) Primitive GEANT4 Event Actioner

(d) Primitive GEANT4 Data Writing

Figure 3: Primitive GEANT4 neutrino imaging code

6 Analysis of Results

In the below results, it is seen that for ν_e different high energy levels for attenuation and absorption, we get the same result for human tissue, which is 0 total energy absorbed at any tissue, either male or female. Such as, male genitalia is, by default, specified as a sensitive tissue, and the uterus, also defined as a sensitive tissue, gives 0 MeV as the energy deposited in the tissue.

Therefore the stated mathematics in Chapter 4 is proven. Interaction is impossible for small masses and volumes with human-tissue-like structures. [7] states that the upper limit for neutrino absorption tomography is 10 TeV. The simulation shows that even in 10 TeV, human-like geometry and tissues are non-interacting with the neutrinos.

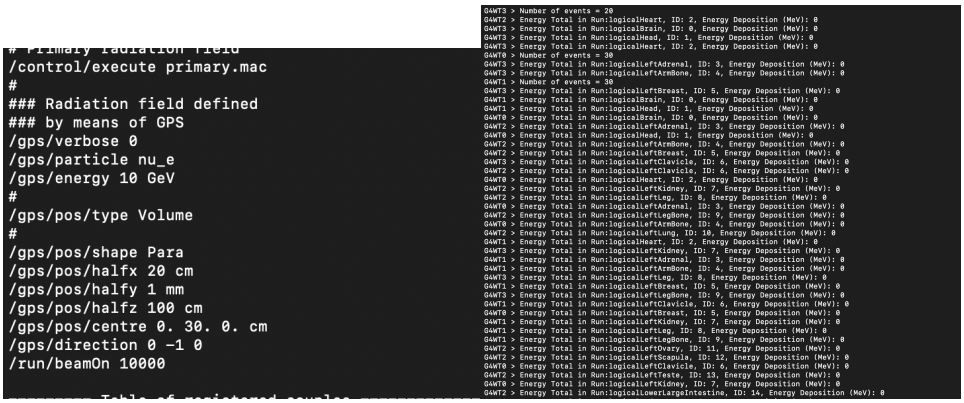

(a) 10 GeV Macro (b) 10 GeV Tissue Energy Depositions

Figure 4: 10 GeV ν_e Simulation

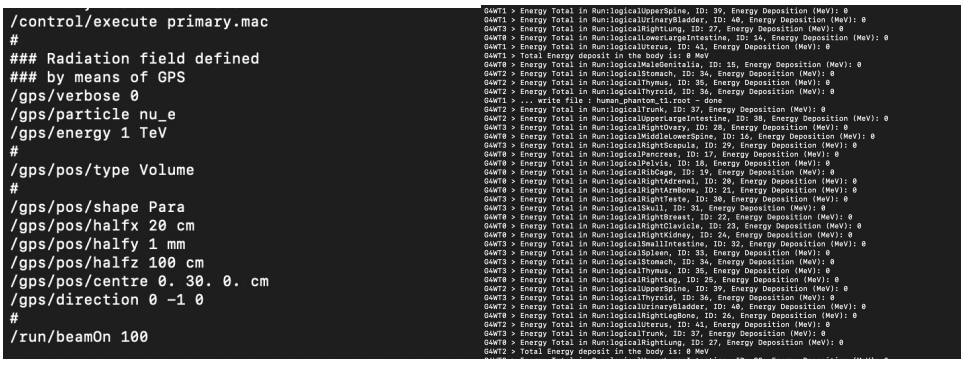

(a) 1 TeV Macro (b) 1 TeV Tissue Energy Depositions

Figure 5: 1 TeV ν_e Simulation

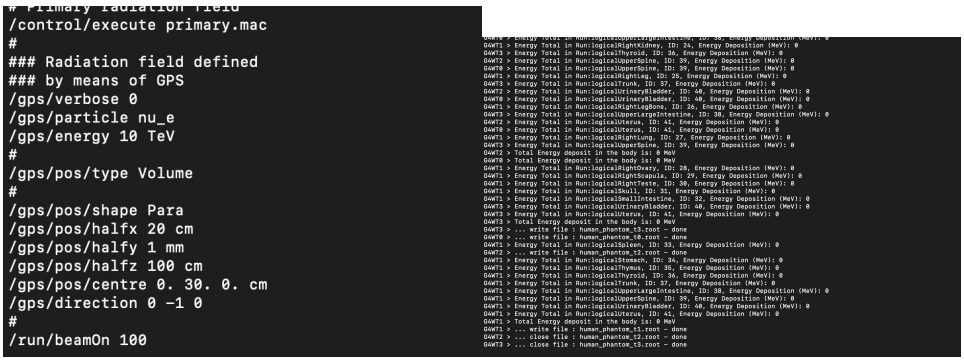

(a) 01 TeV Macro (b) 10 TeV Tissue Energy Depositions

Figure 6: 10 TeV ν_e Simulation

7 Discussion and Conclusion

In conclusion, our work investigates the neutrino's role in non-invasive medical diagnostics using neutrino absorption simulations. Even though neutrinos are weakly interacting with matter, their cross-sections increase as energy increases. Also, the improvements in the neutrino detection systems reveal a possibility for practical applications of neutrino tomography. Its use in nuclear security and earth density reconstruction has recently been discussed. Upon these advancements, we simulated the absorption of neutrinos through a soft tissue-like material in Geant4. Our findings suggest that neutrino absorption is very small. Thus, neutrino absorption tomography is not practically applicable to the considered energy range in human imaging. One may consider the usage of neutrinos in celestial imaging, which has been discussed in academia in recent years. It is also possible to develop a more advanced human phantom for future imaging developments and video visualization and data plotting.

8 References

[1] M. Sajjar-Athar, A. Fatima, and S. K. Singh, "Neutrinos and their interactions with matter" Eur. Phys. J. Spec. Top. **230**, 011003 (2021) doi:10.1140/epjs/s11734-021-00302-x [hep-ph/13792].

[2] L. Livieratos, "Basic Principles of SPECT and PET Imaging", *Radionuclide and Hybrid Bone Imaging*, Springer **345-359** (2012) doi:10.1007/978-3-642-02400-9-12 [hep-ph/13792].

[3] A. Bernstein *et al.*, "Colloquium: Neutrino detectors as tools for nuclear security", Rev. Mod. Phys. **92**, 011003 (2020) doi:10.1103/RevModPhys.92.011003 [hep-ph/9810457].

[4] T. Asaka *et al.*, "Tomography by neutrino pair beam", J. Phys. Let. B **785**, 115004 (2018) doi:10.1016/j.physletb.2018.09.004 [hep-ph/1805.10793].

[5] J. C. D'Olivo, J. A. Herrera-Lara, I. Romero, *et al.,* "Earth tomography with atmospheric neutrino oscillations", Eur. Phys. J. C. **80**, 10052 (2020) doi:10.1140/epjc/s10052-020-08585-5

[6] J. C. D'Olivo, J. A. Herrera-Lara, I. Romero, *et al.,* "Oscillation tomography study of Earth's composition and density with atmospheric neutrinos", Eur. Phys. J. C. **82**, 10052 (2022) doi:10.1140/epjc/s10052-022-10563-y [physics.geo-ph/11257].

[7] W. Walter, "Neutrino tomography - Learning about the Earth's interior using the propagation of neutrinos", Earth Moon Planet **99**, 0602049 (2006) doi:10.1007/s11038-006-9101-y [physics.geo-ph/0602049].

[8] A. Donini, S. Palomares-Ruiz and J. Salvado, "Neutrino tomography of Earth", Nature Phys. **15**, 05901 (2019) doi:10.1038/s41567-018-0319-1 [hep-ph/05901].

[9] T. Akindele *et al.,* "Nu Tools: Exploring Practical Roles for Neutrinos in Nuclear Energy and Security", U.S. Department of Energy Office of Scientific and Technical Information (2021) doi:10.2172/1826602 [hep-ph/12593].

[10] M. Apollonio, A. Baldini, C. Bemporad, *et al.,* "Limits on neutrino oscillations from the CHOOZ experiment", J. Phys. Let. B, **415-430** (1999) doi:10.1016/s0370-2693(99)01072-2. [hep-ex/9907037]

[11] B. R. Martin, "Nuclear and Particle Physics an Introduction.", Hoboken, N.J: John Wiley & Sons, (2009)